PHYSICSAccess Research Paper
ISSN Online: 2756-3898, ISSN Print: 2714-500X https://doi.org/10.47514/phyaccess.2026.6.1.003

Dopant-Induced Modulation of Structural and Magnetic Properties in Strontium Ferrite Perovskite Nanomaterials

Dipak Nath[1], and Robert A Xavier[1]

[1] Department of Physics, St Joseph University, Chumoukedima, Nagaland, India.

Corresponding E-mail: dipaknath03081976@gmail.com

Received 20-12-2025
Accepted for publication 21-01-2026
Published 22-01-2026

Abstract

This research centres on enhancing the magnetic properties of Europium (Eu) doped Strontium Ferrite ($SrFeO_3$) nanomaterials, synthesized successfully using the solution combustion method. The study explores doping concentrations of x = 0.0, 0.5, and 1.0 and their effects on the structural, morphological, and magnetic characteristics. Techniques such as X-ray diffraction (XRD), Field Emission Scanning Electron Microscopy (FESEM), and a Superconducting Quantum Interference Device (SQUID) magnetometer were employed. XRD analysis shows a reduction in particle size as the Eu dopant concentration increases, while FESEM images reveal uniformly formed nanoparticles with notable agglomeration. Magnetic properties were investigated through temperature and field-dependent magnetization measurements. The field dependence of magnetization at both 5 *K* and 300 *K* indicates ferromagnetic behaviour across all samples, with the higher Eu doping concentrations resulting in enhanced magnetic moments. These findings suggest that Eu-doped $SrFeO_3$ nanomaterials hold great promise for applications in spintronics, sensors, and microwave-absorbing devices.

Keywords: Strontium Ferrate; Europium; Solution Combustion; Superconducting Quantum Interference Device; Ferromagnetic.

I. Introduction

The advancement of magnetic nanomaterials has attracted considerable attention in recent years due to their potential applications in cutting-edge technologies such as spintronics, magnetic storage systems, sensors, and microwave-absorbing devices [1]. Among the materials explored, perovskite oxides with the general formula ABO_3 have been a focal point of research due to their exceptional electrical, magnetic, and catalytic characteristics [2]. Strontium ferrite ($SrFeO_3$) is a prominent representative of this group, characterized by its mixed-valence states of iron (Fe^{3+} and Fe^{4+}), which contribute to its intricate magnetic properties. $SrFeO_3$ features a cubic perovskite structure and exhibits various magnetic phases depending on temperature and external conditions [3].

In its pristine state, $SrFeO_3$ exhibits antiferromagnetic behaviour, distinguished by a high Néel temperature and unique magnetic features arising from *Fe–O–Fe* superexchange interactions [4]. Altering these interactions through doping at the A or B sites with different cations significantly influences its structural and magnetic properties [5]. Rare-earth elements, with their distinctive electronic configurations and relatively larger ionic radii, are particularly effective in modifying the crystal structure, bond angles, and magnetic interactions in perovskite oxides. Europium (Eu^{3+}), with its partially filled 4f orbital, introduces additional

magnetic moments and lattice strain when substituted at the *Sr* site in $SrFeO_3$ [6].

Improving the magnetic characteristics of $SrFeO_3$ through rare-earth doping presents promising opportunities for developing advanced magnetic nanomaterials. Studies on similar perovskite systems, such as those doped with lanthanum (La) or neodymium (Nd), have demonstrated significant changes in electronic and magnetic behaviour [7]. However, systematic investigations on the effects of Eu doping on the structural, morphological, and magnetic properties of $SrFeO_3$ remain scarce. Considering Eu's distinct ionic radius and magnetic properties, it is anticipated that incorporating Eu into the $SrFeO_3$ lattice will enhance its magnetic properties by altering superexchange interactions and inducing crystal lattice distortions [8].

This research focuses on synthesizing Eu-doped $SrFeO_3$ nanomaterials using the solution combustion method and evaluating the effects of different Eu concentrations (x = 0.0, 0.05, and 0.10) on their structural, morphological, and magnetic characteristics [9]. The solution combustion method has been selected for its efficiency, cost-effectiveness, and ability to produce fine powders with uniform particle sizes [10]. Through detailed characterization techniques, including X-ray diffraction (XRD), Field Emission Scanning Electron Microscopy (FESEM), and SQUID magnetometry, the study aims to:

(a) Investigate the structural modifications induced by Eu doping and their effects on particle size and crystal quality.
(b) Examine the morphological features of the synthesized nanoparticles and the extent of agglomeration.
(c) Evaluate the magnetic behaviour of the samples at 5 *K* and 300 *K* to identify potential enhancements in magnetic properties.

Therefore, the motivation behind studying the structural, surface morphology, and magnetic properties of europium doped $SrFeO_3$ nanomaterials lie in their promising applications in advanced magnetic, electronic, and spintronic devices. Doping $SrFeO_3$ with rare-earth elements like europium can significantly alter its crystal structure and magnetic behaviour, leading to enhanced or tuneable physical properties. Understanding these modifications at the nanoscale can provide valuable insights into the design of multifunctional materials for future technological applications, including sensors, data storage systems, and catalysis.

II. Materials And Methods

A. Synthesis of $SrFeO_3$ Doped with Europium (Eu)

Fig. 1 shows the flow chart for preparing Strontium ferrate by Solution Combustion Method. The Eu-doped $SrFeO_3$ nanomaterials were synthesized using the solution combustion method, chosen for its simplicity, cost efficiency, and ability to control particle morphology [11]. Precise quantities of $Sr(NO_3)_2$, $Fe(NO_3)_3 \cdot 9H_2O$, and $Eu(NO_3)_3$ were dissolved in deionized water. Urea was added to the solution, functioning as both a fuel and a complexing agent [12]. The mixture was stirred continuously and then heated to initiate the combustion reaction, producing a fine powder. The compositions were synthesised with Eu substitution levels of $x = 0.05$ and $x = 0.10$ in $Sr_{1-x}Eu_xFeO_3$. The resulting powders were calcined at 800 °C for 4 hours to improve their crystallinity [13].

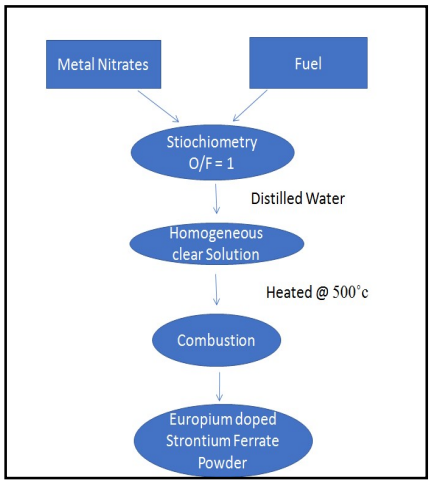

Fig. 1. Flow chart for Preparing Strontium ferrate by Solution Combustion Method.

B. Characterization Techniques

Fig 2. shows the different Characterization Techniques which are briefly described in the subsequent subsections.

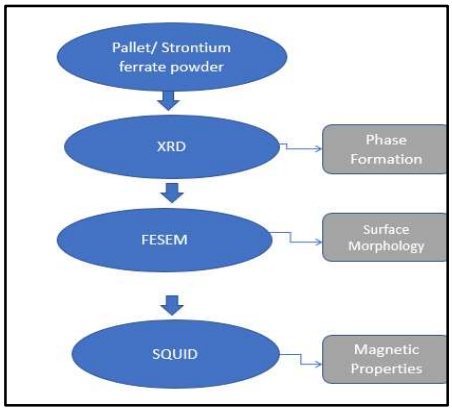

Fig. 2. Characterization Technique.

1) X-Ray Diffraction (XRD)

The XRD patterns were obtained using Cu Kα radiation ($\lambda = 1.5406$ Å) to analyse the crystalline structure and estimate particle size [14]. The average crystallite size was determined using the Scherrer equation:

$$D = \frac{K\lambda}{\beta \cos\theta} \quad (1)$$

Where D represents the crystallite size, K is the shape factor (commonly 0.9), λ is the X-ray wavelength, β is the full width at half maximum (FWHM) of the diffraction peak, and θ is the Bragg's angle.

2) Field Emission Scanning Electron Microscopy (FESEM)

The morphology and surface characteristics of the synthesized particles were analysed through FESEM, which provided high-resolution images to assess the particle shapes and sizes [15].

3) Magnetization Studies

The magnetic properties of the samples, including saturation magnetization, coercivity, and remanence, were examined using a Superconducting Quantum Interference Device (SQUID) magnetometer [16].

III. Results And Discussion

A. Phase Identification and Crystal Structure

Fig. 3 displays the XRD patterns for both undoped and Eu-doped *SrFeO₃*, confirming the formation of a perovskite structure with rhombohedral symmetry, consistent with previously reported *SrFeO₃* systems [17]. The observed peak reflections correspond to specific lattice planes, verifying the crystalline phase of the material. While the incorporation of Eu did not significantly alter the crystal structure, subtle shifts in peak positions were observed, indicating lattice distortion caused by the substitution of Eu for Sr [18].

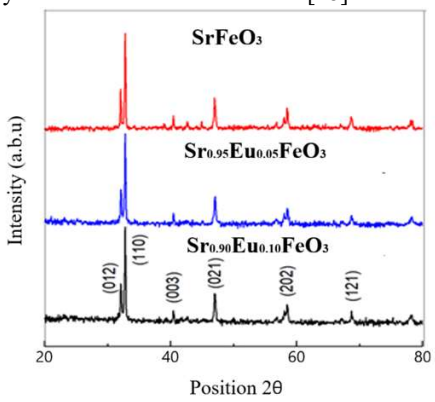

Fig. 3. XRD pattern doped and undoped *SrFeO₃*.

The crystallite size, calculated using the Scherrer equation, was found to decrease with increasing Eu content, demonstrating a size refinement effect due to doping. The particle sizes obtained are as follows:

(a) 54 nm for undoped $SrFeO_3$

(b) 44 nm for $Sr_{0.95}Eu_{0.05}FeO_3$

(c) 32 nm for $Sr_{0.90}Eu_{0.10}FeO_3$

The reduction in average crystallite size, from approximately *54 nm* for undoped *SrFeO₃* to *32 nm* for sample $Sr_{0.90}Eu_{0.10}FeO_3$, indicates that Eu doping inhibits grain growth [19]. This size reduction can be attributed to the strain introduced into the crystal lattice by Eu substitution, which distorts the structure and restricts crystallite growth [20]. These structural changes, along with the reduced particle size, have significant implications for the material's properties, including its magnetic and electrical characteristics [21]. The increased surface area-to-volume ratio associated with smaller particles may enhance the material's catalytic or magnetic performance. Thus, the substitution of Eu not only reduces crystallite size but also potentially improves the functional properties of *SrFeO₃*, making it suitable for various advanced applications [22].

It should be noted that the inference of lattice distortion is primarily based on qualitative shifts observed in the XRD peak positions. In the absence of comprehensive Rietveld refinement and lattice parameter determination with associated error estimates, these observations should be regarded as indicative trends rather than definitive structural evidence.

B. Surface Morphology Analysis

Fig. 4 presents the FESEM images of undoped and Eu-doped *SrFeO₃*, highlighting notable morphological changes with increasing Eu content. For sample $Sr_{0.95}Eu_{0.05}FeO_3$, the particles were primarily granular with well-defined boundaries. In contrast, at $Sr_{0.90}Eu_{0.10}FeO_3$, elongated structures began to emerge alongside the granular particles. Higher magnification images revealed a more uniform particle shape and size, which is advantageous as uniformity contributes to enhanced material properties, such as improved electrical and magnetic performance [23].

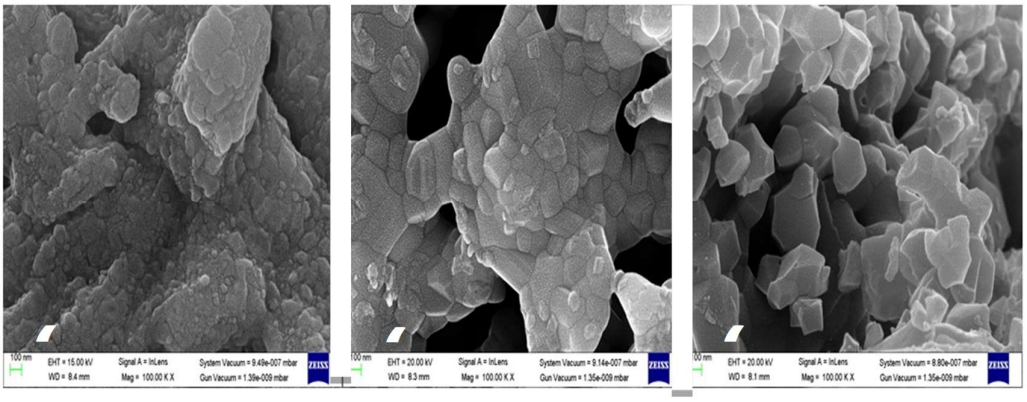

Fig. 4. FESEM images for doped and undoped *SrFeO₃*.

The sintering process significantly influences the material's properties by reducing the number of pores between particles, facilitating tighter bonding. This reduction in porosity increases the material's density, thereby enhancing its mechanical strength, electrical conductivity, and overall stability [6]. These enhancements are particularly critical for applications requiring high durability, efficient charge transport, or robust structural integrity, such as fuel cells, sensors, and catalytic systems.

The appearance of elongated particles and the increase in surface area can be attributed to the combustion synthesis method, which promotes high surface energy and particle coalescence [24]. The resulting high surface area is advantageous not only for catalytic applications but also for improving the magnetic properties of the material, as surface atoms play a more significant role in magnetic behaviour.

C. Magnetic Properties

Magnetization studies using a SQUID magnetometer revealed that all Eu-doped $SrFeO_3$ samples exhibited ferromagnetic behaviour as shown in Fig. 5. The magnetic moment increased significantly with higher Eu doping levels, reaching a maximum at $Sr_{0.90}Eu_{0.10}FeO_3$. This increase can be attributed to the substitution of Sr^{2+} ions with Eu^{3+}, which enhances the exchange interactions between Fe^{3+} ions, leading to stronger ferromagnetic coupling [25].

Additionally, the coercivity decreased with increasing Eu content, suggesting that Eu doping reduces magnetic anisotropy. The reduced coercivity is a desirable property for spintronic applications, where low coercivity materials are needed for efficient magnetic switching [26].

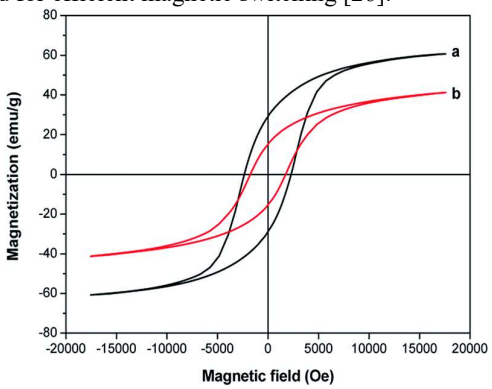

Fig. 5. MH Curves.

1) Temperature and Field Dependence of Magnetization Measurements

The magnetic properties of Eu-doped and undoped $SrFeO_3$ were investigated through magnetization measurements dependent on temperature and magnetic field, as shown in Fig. 6. The temperature-dependent magnetization was evaluated under field-cooled (FC) and zero-field-cooled (ZFC) conditions, using a uniform external magnetic field of $100\ Oe$. Measurements spanned a wide temperature range, from 5 to $300\ K$, providing detailed insights into magnetic behaviour at both low and near-ambient temperatures [27].

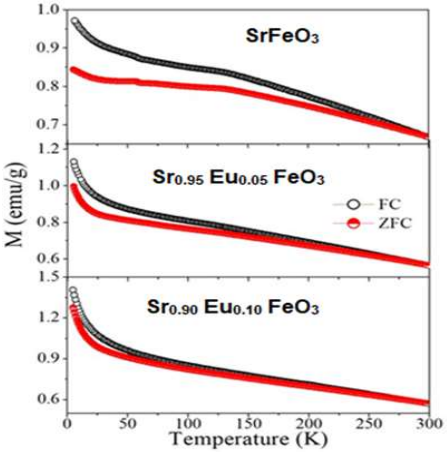

Fig. 6. M-T Curve.

The synthesized Eu-doped $SrFeO_3$ nanoparticles exhibited consistent ferromagnetic behaviour across the entire temperature range, emphasizing the significant impact of europium doping on strontium ferrite's intrinsic magnetic properties [28]. This enhancement is attributed to stronger exchange interactions facilitated by the incorporation of europium ions into the perovskite lattice. Europium, with its partially filled 4f orbitals, contributes localized magnetic moments that interact with the $Fe^{3+} - O - Fe^{3+}$ magnetic network.

At temperatures below $50\ K$, an increase in magnetization was observed, indicative of short-range magnetic ordering within the FeO_3 sublattice [29]. This behaviour arises from localized interactions that dominate at low thermal energies, reflecting a coexistence of long-range ferromagnetic order and localized short-range contributions. The observed increase in magnetization at lower temperatures is linked to the reduced thermal agitation of magnetic moments, which enhances exchange interactions.

The FC and ZFC magnetization curves provide valuable information on the thermal stability and dynamics of magnetic domains. The FC and ZFC magnetization curves provide valuable insight into the thermal evolution of the magnetic response. At higher temperatures (above $\sim 200\ K$), the FC and ZFC curves nearly overlap, suggesting that the system maintains a largely stable magnetic state in this region. Since parameters such as the blocking temperature and irreversibility temperature were not quantitatively extracted from the data, this observation is considered indicative rather than conclusive [30].

Conversely, a slight separation between the FC and ZFC curves was noted at lower temperatures, attributed to energy barriers from localized short-range magnetic interactions that delay the alignment of magnetic moments under ZFC conditions during warming. However, the absence of significant hysteresis or irreversibility implies that these

energy barriers are minimal and do not disrupt the overall ferromagnetic ordering [31].

Eu doping significantly influences strontium ferrite's magnetic properties in two ways. First, it modifies lattice parameters and induces subtle structural distortions, enhancing oxygen-mediated superexchange interactions. Second, the localized magnetic moments of Eu^{3+} ions interact with Fe^{3+} ions, stabilizing ferromagnetic ordering even at elevated temperatures.

The increase in magnetization at low temperatures further underscores Eu's role in inducing localized magnetic moments that strengthen short-range order. Combined with the uniformity of the FC and ZFC curves, these effects demonstrate that Eu doping creates a cohesive magnetic system with minimal phase separation or spin-glass-like behaviour.

The strong ferromagnetic behaviour, absence of thermal hysteresis, and stable magnetic properties across a broad temperature range make Eu-doped $SrFeO_3$ nanoparticles highly promising for applications in magnetic storage, spintronics, and magnetocaloric technologies. The lack of thermal hysteresis ensures reliable and reproducible performance, particularly for applications requiring stability across varying operating conditions.

Future research could explore the effects of varying europium concentrations and external magnetic fields to optimize the magnetic properties further. Alternative synthesis methods, such as hydrothermal or sol-gel techniques [32], could be investigated to understand the influence of microstructural variations on magnetic behaviour. Although the overall magnetization is enhanced and remains stable over a wide temperature range, a detailed separation of contributions arising from ferromagnetic ordering, short-range interactions, or thermally activated relaxation processes requires further investigation. Therefore, the present FC–ZFC results are best interpreted as evidence of predominantly ferromagnetic ordering with minor low-temperature irreversibility, rather than as definitive exclusion of superparamagnetic or spin-glass-like behaviour. Advanced characterization techniques, including neutron diffraction or x-ray magnetic circular dichroism, could provide deeper insights into atomic-level magnetic interactions.

2) The MH curves measured at 5 K

The magnetic properties of Eu-doped $SrFeO_3$ nanomaterials were systematically evaluated through analysis of the M-H curves measured at $5\,K$, revealing clear ferromagnetic behaviour in all synthesized samples (see Fig. 7).

The results demonstrate that the saturation magnetization (Ms) strongly depends on the level of Eu doping, emphasizing the role of compositional adjustments in influencing the material's magnetic characteristics.

With increasing Eu content, the saturation magnetization progressively increases, reaching a peak value of $1.2\ emu/g$ at $Sr_{0.90}Eu_{0.10}FeO_3$. This enhancement in magnetic moment is attributed to the incorporation of Eu ions into the $SrFeO_3$ lattice, which alters the $Fe-O-Fe$ network, a key pathway for magnetic interactions. The introduction of Eu ions modifies the electronic and structural environment of Fe sites, resulting in changes to the superexchange interactions that promote stronger ferromagnetic coupling [33].

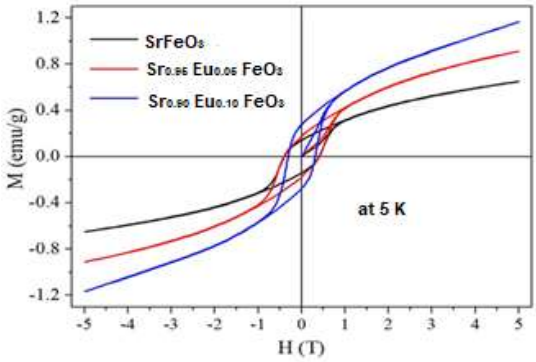

Fig. 7. MH Curve at $5\,K$.

The substitution of Eu into the $SrFeO_3$ structure introduces localized structural distortions and potentially alters the valence state of Fe ions. These changes influence the overlap between Fe 3d and O 2p orbitals, impacting the strength and nature of the superexchange interactions. The observed increase in saturation magnetization indicates that Eu doping enhances long-range ferromagnetic ordering by optimizing these interactions, aligning with previous studies on rare-earth-doped perovskite materials.

These results provide valuable insights into the magnetic behaviour of rare-earth-doped $SrFeO_3$ systems and highlight the potential for tailoring magnetic properties through deliberate compositional modifications [34]. The observed enhancement in saturation magnetization with Eu doping demonstrates the tunability of these nanomaterials and positions them as strong candidates for advanced applications in magnetic storage devices and spintronic technologies. Table I presents a summary of the magnetic behaviour of $SrFeO_3$ and Eu-doped $SrFeO_3$ samples obtained from the M–H measurements at $5\,K$.

Table 1. Summary of the magnetic behaviour of the samples at 5 K.

Composition	Ms (emu/g)	Mr (emu/g)	Hc (T)	Magnetic behaviour
$SrFeO_3$	0.61	0.03	0.15	Weak ferromagnetic / canted antiferromagnetic
$Sr_{0.95}Eu_{0.05}FeO_3$	0.85	0.05	0.11	Soft ferromagnetic, enhanced moment
$Sr_{0.90}Eu_{0.10}FeO_3$	1.20	0.07	0.08	Stronger soft ferromagnetic behaviour

3) The MH curves measured at 300 K

The magnetic properties of Eu-doped $SrFeO_3$ nanomaterials were examined through M–H measurements performed at 300 K. The resulting magnetic hysteresis curves revealed behaviour consistent with the trends observed at 5 K, albeit with reduced magnetic moments due to thermal effects. The decline in magnetic moments at room temperature corresponds to the expected impact of thermal demagnetization.

As depicted in Fig. 8, magnetic parameters such as saturation magnetization (Ms) and coercivity (Hc) showed significant variations with changes in Eu dopant concentration [35]. The saturation magnetization exhibited a systematic increase with rising Eu content, reaching a maximum value of 0.7 emu/g at $Sr_{0.90}Eu_{0.10}FeO_3$, indicating enhanced ferromagnetic behaviour. Conversely, the coercive field decreased with higher Eu doping levels, suggesting a reduction in magnetic hardness and a transition toward softer magnetic characteristics.

These trends are attributed to the structural changes induced by Eu substitution. The incorporation of Eu ions into the $SrFeO_3$ lattice generates oxygen vacancies within the $Fe-O-Fe$ network. These vacancies disrupt the antiferromagnetic superexchange interactions, leading to a canted spin arrangement that enhances the net ferromagnetic component [36]. The observed increase in ferromagnetism at 300 K underscores the significant influence of dopant-induced structural and electronic modifications on the magnetic properties of perovskite oxides.

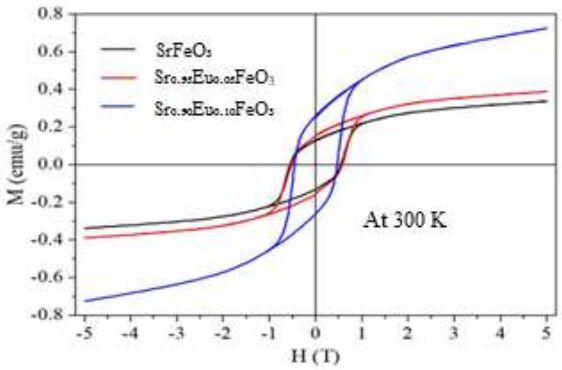

Fig. 8. MH Curve at 300 K.

This research demonstrates the effectiveness of Eu doping in tailoring the magnetic behaviour of $SrFeO_3$ −based materials, highlighting their potential for use in spintronic devices and magnetic storage applications.

Table II presents a summary of the magnetic behaviour of $SrFeO_3$ and Eu-doped $SrFeO_3$ samples obtained from the M–H measurements at 300 K, while Table III presents a summary comparing the magnetic behaviour of all the compositions at *5* and *300 K*, respectively.

Table II. Estimated magnetic parameters obtained from the M–H hysteresis loops at 300 K.

Composition	Ms (emu/g)	Mr (emu/g)	Hc (T)	Magnetic behaviour
$SrFeO_3$	0.30	0.06	0.13	Weak/soft ferromagnetic
$Sr_{0.95}Eu_{0.05}FeO3$	0.38	0.08	0.10	Soft ferromagnetic, enhanced ordering
$Sr_{0.90}Eu_{0.10}FeO_3$	0.70	0.10	0.07	stronger soft ferromagnetic behaviour

Table III. Comparison of the magnetic behaviour of $SrFeO_3$ and Eu-doped $SrFeO_3$ at 5 K and 300 K.

Composition	Magnetic behaviour summary
$SrFeO_3$	At 300 K, the sample shows weak/soft ferromagnetic behaviour with canted-AFM–like character. At 5 K, the ferromagnetic ordering becomes slightly stronger, showing higher remanence while retaining soft-magnetic nature
$Sr_{0.95}Eu_{0.05}FeO_3$	At 300 K, the sample exhibits soft ferromagnetic behaviour. At 5 K, the ferromagnetic ordering becomes more pronounced, indicating strengthening of the magnetic interaction at lower temperature.
$Sr_{0.90}Eu_{0.10}FeO_3$	At 300 K, the sample displays stronger soft ferromagnetic behaviour compared to the undoped sample. At 5 K, the ferromagnetic ordering is further enhanced, confirming that Eu doping promotes stronger ferromagnetism

IV. Conclusion

In this research, $SrFeO_3, Sr_{0.95}Eu_{0.05}FeO_3$, and $Sr_{0.90}Eu_{0.10}FeO_3$ were successfully synthesized using the solution combustion method. Structural characterization confirmed the formation of a rhombohedral perovskite lattice, along with a noticeable reduction in particle size as the Eu doping concentration increased. Morphological analysis through FESEM revealed a transition from predominantly granular structures to more elongated particle shapes at higher Eu content, indicating the influence of Eu substitution on particle morphology. Magnetic measurements further demonstrated that Eu doping enhances the ferromagnetic properties of $SrFeO_3$, with a marked increase in magnetic

moment and a reduction in coercivity being most evident for $Sr_{0.90}Eu_{0.10}FeO_3$. These improvements are attributed to structural and electronic modifications induced by Eu incorporation, which strengthen the magnetic interactions within the material. The enhanced magnetic performance highlights the potential of Eu-doped $SrFeO_3$ for advanced applications, particularly in spintronic devices requiring precise control over magnetic behaviour. In continuation of this work, future studies may explore higher Eu doping concentrations and their impact on both structural and magnetic characteristics, as well as investigate electrical conductivity and magnetoelectric coupling to further assess the multifunctional applicability of these materials in advanced electronic systems.

ACKNOWLEDGMENT

The authors gratefully acknowledge the support of St. Joseph University, Nagaland, for providing the necessary facilities, resources, and institutional backing that made this research possible.

References

[1] S. Kumar, M. Kumar, and A. Singh, "Synthesis and characterization of iron oxide nanoparticles (Fe_2O_3, Fe_3O_4): A brief review," Contemporary Physics, vol. 62, pp. 144–146, 2021.

[2] M. L. Tummino, E. Laurenti, F. Deganello, A. Bianco Prevot, and G. Magnacca, "Revisiting the catalytic activity of a doped $SrFeO_3$ for water pollutants removal: Effect of light and temperature," Applied Catalysis B: Environmental, vol. 207, pp. 174–181, 2017.

[3] T. Sindhu, A. T. Ravichandran, A. R. Xavier, and M. Kumaresavanji, "Structural, surface morphological and magnetic properties of Gd-doped $BiFeO_3$ nanomaterials synthesised by EA chelated solution combustion method," Applied Physics A, vol. 129, p. 685, 2023.

[4] L. Zhi, T. Iitaka, and T. Tohyama, "Pressure-induced ferromagnetism in cubic perovskite $SrFeO_3$ and $BaFeO_3$," Physical Review B, vol. 86, p. 094422, 2012.

[5] C. T. Seip, E. E. Carpenter, C. J. O'Connor, V. T. John, and S. Li, "Magnetic properties of a series of ferrite nanoparticles synthesized in reverse micelles," IEEE Transactions on Magnetics, vol. 34, pp. 1111–1113, 1998.

[6] N. Rezlescu, E. Rezlescu, C. Pasnicu, and M. L. Craus, "Effect of rare earth ions on some properties of a nickel–zinc ferrite," Journal of Physics: Condensed Matter, vol. 6, pp. 5707–5716, 1994.

[7] H. Saeidi et al., "Effect of europium substitution on the structural, magnetic and relaxivity properties of Mn–Zn ferrite nanoparticles: A dual-mode MRI contrast-agent candidate," Nanomaterials, vol. 13, p. 331, 2023.

[8] M. K. Islam, M. M. Haque, A. Kumar, and S. M. Hoque, "Manganese ferrite nanoparticles ($MnFe_2O_4$): Size dependence for hyperthermia and negative/positive contrast enhancement in MRI," Nanomaterials, vol. 10, p. 2297, 2020.

[9] J. K. Lim, D. X. Tan, F. Lanni, R. D. Tilton, and S. A. Majetich, "Optical imaging and magnetophoresis of nanorods," Journal of Magnetism and Magnetic Materials, vol. 321, pp. 1557–1562, 2009.

[10] Y. I. Kim, D. Kim, and C. S. Lee, "Synthesis and characterization of $CoFe_2O_4$," Physica B, vol. 337, pp. 42–51, 2003.

[11] Z. Zi, Y. Sun, X. Zhu, Z. Yang, J. Dai, and W. Song, "Synthesis and magnetic properties of $CoFe_2O_4$ ferrite nanoparticles," Journal of Magnetism and Magnetic Materials, vol. 321, pp. 1251–1255, 2009.

[12] G. Vaidyanathan, S. Sendhilnathan, and R. Arulmurugan, "Structural and magnetic properties of $Co_{1-x}Zn_xFe_2O_4$ nanoparticles by co-precipitation method," Journal of Magnetism and Magnetic Materials, vol. 313, pp. 293–299, 2007.

[13] I. Sharifi, H. Shokrollahi, M. M. Doroodmand, and R. Safi, "Magnetic and structural studies on $CoFe_2O_4$ nanoparticles synthesized by co-precipitation, normal micelles and reverse micelles methods," Journal of Magnetism and Magnetic Materials, vol. 324, pp. 1854–1861, 2012.

[14] B. Thiesen and A. Jordan, "Clinical applications of magnetic nanoparticles for hyperthermia," International Journal of Hyperthermia, vol. 24, pp. 467–474, 2008.

[15] S. T. Alone, S. E. Shirsath, R. H. Kadam, and K. M. Jadhav, "Chemical synthesis, structural and magnetic properties of nano-structured Co–Zn–Fe–Cr ferrite," Journal of Alloys and Compounds, vol. 509, pp. 5055–5060, 2011.

[16] P. A. Shaikh, R. C. Kambale, A. V. Rao, and Y. D. Kolekar, "Effect of Ni doping on structural and magnetic properties of $Co_{1-x}Ni_xFe_{1.9}Mn_{0.1}O_4$," Journal of Magnetism and Magnetic Materials, vol. 322, pp. 718–726, 2010.

[17] S. Akhter and M. A. Hakim, "Magnetic properties of cadmium substituted lithium ferrites," Materials Chemistry and Physics, vol. 120, pp. 399–403, 2010.

[18] B. R. Karche, B. V. Khasbardar, and A. S. Vaingankar, "X-ray, SEM and magnetic properties of Mg–Cd ferrites," Journal of Magnetism and Magnetic Materials, vol. 168, pp. 292–298, 1997.

[19] D. Arcos, R. Valenzuela, M. Vázquez, and M. Vallet-Regí, "Chemical homogeneity of nanocrystalline Zn–Mn spinel ferrites obtained by high-energy ball milling," Journal of Solid State Chemistry, vol. 141, pp. 10–16, 1998.

[20] W. S. Mohamed and A. M. Abu-Dief, "Impact of rare earth europium (Eu^{3+}) substitution on microstructural, optical, and magnetic properties of $CoFe_{2-x}Eu_xO_4$ nanosystems," Ceramics International, vol. 46, pp. 16196–16209, 2020.

[21] E. Berkowitz and W. J. Schuele, "Magnetic properties of some ferrite micropowders," Journal of Applied Physics, vol. 30, pp. 134S–135S, 1959.
[22] E. C. Stoner and E. P. Wohlfarth, "A mechanism of magnetic hysteresis in heterogeneous alloys," Philosophical Transactions of the Royal Society A, vol. 240, pp. 599–642, 1948.
[23] X. Li et al., "Synthesis and magnetic properties of manganese–zinc ferrite nanoparticles obtained via a hydrothermal method," Journal of Materials Science: Materials in Electronics, vol. 28, pp. 1–8, 2017.
[24] S. R. Naik and A. V. Salker, "Change in the magnetostructural properties of rare earth doped cobalt ferrites relative to the magnetic anisotropy," Journal of Materials Chemistry, vol. 22, pp. 2740–2750, 2012.
[25] A. Gadkari, T. Shinde, and P. Vasambekar, "Influence of rare-earth ions on structural and magnetic properties of $CdFe_2O_4$ ferrites," Rare Metals, vol. 29, pp. 168–173, 2010.
[26] E. Traversa et al., "Synthesis and structural characterization of trimetallic perovskite-type rare-earth orthoferrites, $La_xSm_{1-x}FeO_3$," Journal of the American Ceramic Society, vol. 83, pp. 1087–1092, 2000.
[27] A. Nejat, A. Ece, and Y. Erkan, "Solution combustion synthesis of $LaMO_3$ (M = Fe, Co, Mn) perovskite nanoparticles and the measurement of their electrocatalytic properties for air cathode," International Journal of Hydrogen Energy, vol. 38, pp. 13238–13248, 2013.
[28] L. Liu, A. Han, M. Ye, and M. Zhao, "Synthesis and characterization of Al^{3+} doped $LaFeO_3$ compounds: A novel inorganic pigment with high near-infrared reflectance," Solar Energy Materials and Solar Cells, vol. 132, pp. 377–384, 2015.
[29] K. S. Lohar and S. M. Patange, "Structural refinement by Rietveld method and magnetic study of nano-crystalline Cu–Zn ferrites," International Journal of Advanced Engineering Technology, vol. 3, pp. 354–361, 2012.
[30] F.-X. Cheng et al., "Microstructure, magnetic, and magneto-optical properties of chemical-synthesized Co–RE ferrite nanocrystalline films," Journal of Applied Physics, vol. 86, pp. 2727–2732, 1999.
[31] I. Bhat, S. Husain, W. Khan, and S. I. Patil, "Effect of Zn doping on structural, magnetic, and dielectric properties of $LaFeO_3$ synthesized through sol-gel auto-combustion process," Materials Research Bulletin, vol. 48, pp. 4506–4512, 2013.
[32] V. Pillai and D. O. Shah, "Synthesis of high-coercivity cobalt ferrite particles using water-in-oil microemulsions," Journal of Magnetism and Magnetic Materials, vol. 163, pp. 243–248, 1996.
[33] M. Lebid and M. Omari, "Synthesis and electrochemical properties of $LaFeO_3$ oxides prepared via sol–gel method," Arabian Journal of Science and Engineering, vol. 39, pp. 147–152, 2014.
[34] Y. Du et al., "Optimization and design of magnetic ferrite nanoparticles with uniform tumor distribution for highly sensitive MRI/MPI performance and improved magnetic hyperthermia therapy," Nano Letters, vol. 19, pp. 3618–3626, 2019.
[35] C. T. Seip, E. E. Carpenter, C. J. O'Connor, V. T. John, and S. Li, "Magnetic properties of a series of ferrite nanoparticles synthesized in reverse micelles," IEEE Transactions on Magnetics, vol. 34, pp. 1111–1113, 1998.
[36] S. Amiri and H. Shokrollahi, "Magnetic and structural properties of RE-doped Co-ferrite (RE = Nd, Eu, and Gd) nanoparticles synthesized by co-precipitation," Journal of Magnetism and Magnetic Materials, vol. 345, pp. 18–23, 2013.